

Absorption-Line Survey of H_3^+ toward the Galactic Center Sources. III. Extent of Warm and Diffuse Clouds*

Miwa GOTO,¹ Tomonori USUDA,² Thomas R. GEBALLE,³ Nick INDRIOLO,⁴ Benjamin J. MCCALL,⁴
Thomas HENNING,¹ and Takeshi OKA⁵

¹Max-Planck-Institut für Astronomie, Königstuhl 17, D-69117 Heidelberg, Germany
mgoto@mpia.de

²Subaru Telescope, 650, North A'ohoku Place, Hilo, HI 96720, USA

³Gemini Observatory, 670, North A'ohoku Place, Hilo, HI 96720, USA

⁴Department of Astronomy and Department of Chemistry, University of Illinois at Urbana-Champaign,
Urbana, IL 61801-3792, USA

⁵Department of Astronomy and Astrophysics, Department of Chemistry, and Enrico Fermi Institute,
University of Chicago, Chicago, IL 60637, USA

(Received 2010 December 22; accepted 2011 February 8)

Abstract

We present a follow-up observation on Geballe and Oka (2010, ApJ, 709, L70), who found high column densities of H_3^+ ~ 100 pc apart from the Galactic center on the lines of sight to 2MASS J17432173–2951430 (J1743) and 2MASS J17470898–2829561 (J1747). The wavelength coverages on these sightlines have been extended in order to observe two key transitions of H_3^+ — $R(3, 3)^l$ and $R(2, 2)^l$ — which constrain the temperature and density of the environment. The profiles of the H_3^+ $R(3, 3)^l$ line, which is due only to gas in the Galactic center, closely match the differences between the H_3^+ $R(1, 1)^l$ and CO line profiles, just as they do for previously studied sightlines in the Galactic center. Absorption in the $R(2, 2)^l$ line of H_3^+ is present in J1747 at velocities of between -60 and $+100$ km s⁻¹. This is the second clear detection of this line in the interstellar medium after GC IRS 3 in the Central cluster. The temperature of the absorbing gas in this velocity range is 350 K, significantly warmer than that of diffuse clouds in other parts of the Central Molecular Zone. This indicates that the absorbing gas localizes on the Sgr B molecular cloud complex. The warm and diffuse gas revealed by Oka et al. (2005, ApJ, 632, 882) apparently extends to ~ 100 pc, but there is a hint that its temperature is somewhat lower in the line of sight to J1743 than elsewhere in the Galactic center. The observation of H_3^+ toward J1747 is compared with the recent Herschel observation of H_2O^+ toward Sgr B2, and their chemical relation and remarkably similar velocity profiles are discussed.

Key words: Galaxy: center — ISM: clouds — ISM: lines and bands — ISM: molecules

1. Introduction

Studying the interstellar medium in the Galactic center using H_3^+ as an astrophysical probe was initiated by Geballe et al. (1999), who discovered that the Galactic center is the richest reservoir of H_3^+ in the Milky Way. The column density of H_3^+ toward the Galactic center is $> 10^{15}$ cm⁻², higher by an order of magnitude than those in dense molecular clouds (McCall et al. 1999) and in diffuse clouds in the Galactic disk (McCall et al. 2002; Indriolo et al. 2007). Studies of H_3^+ in the interstellar medium initially relied on the vibration-rotation transitions from the two lowest rotational levels: $(J, K) = (1, 1)$ and $(1, 0)$. The first interstellar H_3^+ line from a higher rotational level was discovered by Goto et al. (2002) toward the bright infrared sources GC IRS 3 and GCS 3-2, near the Galactic center. The $(J, K) = (3, 3)$ level from which the observed $R(3, 3)^l$ originates is 361 K above the lowest level, and is “metastable”; that is, H_3^+ in this level does not decay by spontaneous emission (Pan & Oka 1986).

Oka et al. (2005) determined the physical state of the gas toward the bright star GCS 3-2 in the Galactic center based on a steady state calculation of thermalization by Oka and Epp (2004). Their results are as follows: (1) compared to diffuse clouds in the Galactic disk, the gas in the Galactic center producing absorption by H_3^+ has a similar density (≤ 100 cm⁻³), but a much higher temperature (~ 250 K); (2) the path length of the absorbing cloud is at least 30 pc, which means that the cloud occupies a significant portion of the volume of the Galactic center; (3) the cosmic-ray ionization rate of H_2 must be at least 10^{-15} s⁻¹, with the limiting value in effect if the line-of-sight dimension of the absorbing cloud is the full diameter of the Central Molecular Zone of the Galaxy (CMZ) (200 pc; Morris & Serabyn 1996).

Subsequently, Goto et al. (2008) found that the interpretation by Oka et al. (2005) is universal for sightlines toward 8 stars located in the Galactic center and extending from Sgr A* to 30 pc east of Sgr A*. Without exception, all eight sightlines that they observed show strong $R(1, 1)^l$ and $R(3, 3)^l$ absorptions with similar column densities of H_3^+ to that toward GCS 3-2, demonstrating that the warm and diffuse gas is present over a wide region of the CMZ.

* Based on data collected at Subaru Telescope, which is operated by the National Astronomical Observatory of Japan.

Table 1. Journal of observations.

	l [°]	b [°]	L	Lines covered	Exposure [s]	Grating*		Standard	
						ECH	XDP	Name	Spe.
2MASS J17432173–2951430	−1.046	−0.065	3.8	$R(4,4)^l, R(2,2)^l, R(1,1)^u, R(1,0)$	960	−9000	2400	HR 6378	A2 V
				$R(3,3)^l$	480	−200	4000	HR 6378	A2 V
2MASS J17470898–2829561	0.548	−0.059		$R(4,4)^l, R(2,2)^l, R(1,1)^u, R(1,0)$	5400	−9000	2400	HR 6378	A2 V
				$R(3,3)^l$	5400	−200	4000	HR 6378	A2 V

* “ECH” and “XDP” denote the motor settings for the angles of echelle and cross-dispersing gratings in the instrumental unit.

In order to explore a wider region of the CMZ, Geballe and Oka (2010) have undertaken a spectroscopic search, from 170 pc east of Sgr A* to 170 pc west, for bright infrared stars in the Spitzer GLIMPSE catalog (Ramírez et al. 2008) with clean infrared continua, that can serve as background sources for H_3^+ spectroscopy. They have reported strong H_3^+ $R(1,1)^l$ and CO $v = 2-0$ absorption toward two stars thus selected, 2MASS J17432173–2951430 and 2MASS J17470898–2829561 (hereafter J1743 and J1747), located 130 pc west of Sgr A* and 80 pc east, respectively. Their results strongly imply that the warm and diffuse environment revealed by Oka et al. (2005) extends to radii of ~ 100 pc.

In the present study we observed the key $R(3,3)^l$ and $R(2,2)^l$ absorptions toward J1743 and J1747 in order to better determine the properties of these two new sightlines. The distance to the Galactic center is assumed to be 7.6 kpc throughout this paper (Eisenhauer et al. 2005; Nishiyama et al. 2006).

2. Observation and Data Reduction

The spectra of J1743 and J1747 were obtained at the Subaru Telescope on 2010 May 4 UT by the high-resolution infrared camera and spectrograph (IRCS: Kobayashi et al. 2000). The used resolving power was $R = 20000$. The angle settings of the echelle and cross-dispersing gratings were -9000 and 2400 , respectively, in order to cover H_3^+ $R(4,4)^l$ [$3.4548 \mu\text{m}$], $R(2,2)^l$ [$3.6205 \mu\text{m}$], $R(1,0)$ [$3.6685 \mu\text{m}$], and $R(1,1)^u$ [$3.6681 \mu\text{m}$], and were -200 and 4000 , respectively, to cover $R(3,3)^l$ [$3.5337 \mu\text{m}$]. The data were obtained while nodding the telescope along the slit, whose dimensions were $0''.14 \times 6''.7$, so as to be able to easily subtract the thermal sky background. The position of the target was continuously manually centered during the observation to maximize the throughput. The centering was performed with the camera of IRCS observing the L' band, the same wavelength as that of the spectroscopic observation, so as to minimize the differential atmospheric refraction. An early-type spectroscopic standard star, HR 6378 (A2 V, $V = 2.43$), was observed immediately before or after the object observation through a similar airmass. Standard calibration data were obtained in the morning; these included spectroscopic flatfields with the same grating settings. The sky was clear and stable through the night, with the seeing measured being $0''.59$ in the K band. A journal of the observations is given in table 1.

Data reduction was performed as described by Goto et al. (2008). The raw spectrograms were pair-subtracted, flatfielded, and corrected for outlier pixels. One-dimensional

spectra of each of the Galactic center objects and of the standard star were extracted using IRAF¹ aperture extraction package. The spectra of the Galactic center sources were further processed by using custom-written IDL codes for correcting the telluric absorption lines, using the spectra of the standard star. Slight wavelength offsets, differences in airmass, fringes on the continuum, and saw-tooth features produced by different readout channels were simultaneously removed. Wavelength calibration was performed by maximizing the correlation with a model atmospheric transmission curve calculated using ATRAN (Lord 1992), and was better than 1 km s^{-1} . Wavelengths were converted to radial velocities with respect to the local standard of the rest, using the IRAF rv package. Normalized absorption spectra of H_3^+ for J1743 and J1747 are shown in figure 1, together with the H_3^+ and CO spectra from Geballe and Oka (2010).

3. Results

The spectra of H_3^+ $R(1,1)^l$ and the CO $v = 2-0$ $R(0)$ line in Geballe and Oka (2010) are considerably different from each other. Here, we compare in detail the difference spectra of those two lines and the $R(3,3)^l$ line profiles observed here.

In the upper traces of figure 2a, we show the superimposition of the velocity profiles of the H_3^+ $R(1,1)^l$ and CO $R(0)$ lines in J1743 taken from Geballe and Oka (2010), but after rescaling CO $R(0)$ by a factor of 0.2 so that the common absorption components at -60 km s^{-1} , which probably both arise solely in dense molecular gas in the foreground 3 kpc spiral arm, as discussed by e.g., Oka et al. (2005), have roughly the same depth. In J1743 the H_3^+ $R(1,1)^l$ line profile consists of six distinct absorptions at 0, -27 , -60 , -75 , -172 , and -200 km s^{-1} , with a minor substructure in the -172 and 0 km s^{-1} components (Geballe & Oka 2010). The CO $v = 2-0$ line shows only three of these features at -60 , -172 , and -200 km s^{-1} . Perhaps, most remarkably, the CO profile is completely lacking the 0 km s^{-1} component, which is the strongest component in the H_3^+ $R(1,1)^l$ profile. The lower trace in orange (or thin line) represents the difference spectrum of $R(1,1)^l$ and the scaled CO $R(0)$ overlaid with $R(3,3)^l$ from the present study. Despite being at a lower spectral resolution than Geballe and Oka (2010), the $R(3,3)^l$ profile qualitatively reproduces the difference spectrum, showing absorption components at 0 and -75 km s^{-1} as well as extra absorption at

¹ IRAF is distributed by the National Optical Astronomy Observatories, which are operated by the Association of Universities for Research in Astronomy, Inc., under cooperative agreement with the National Science Foundation.

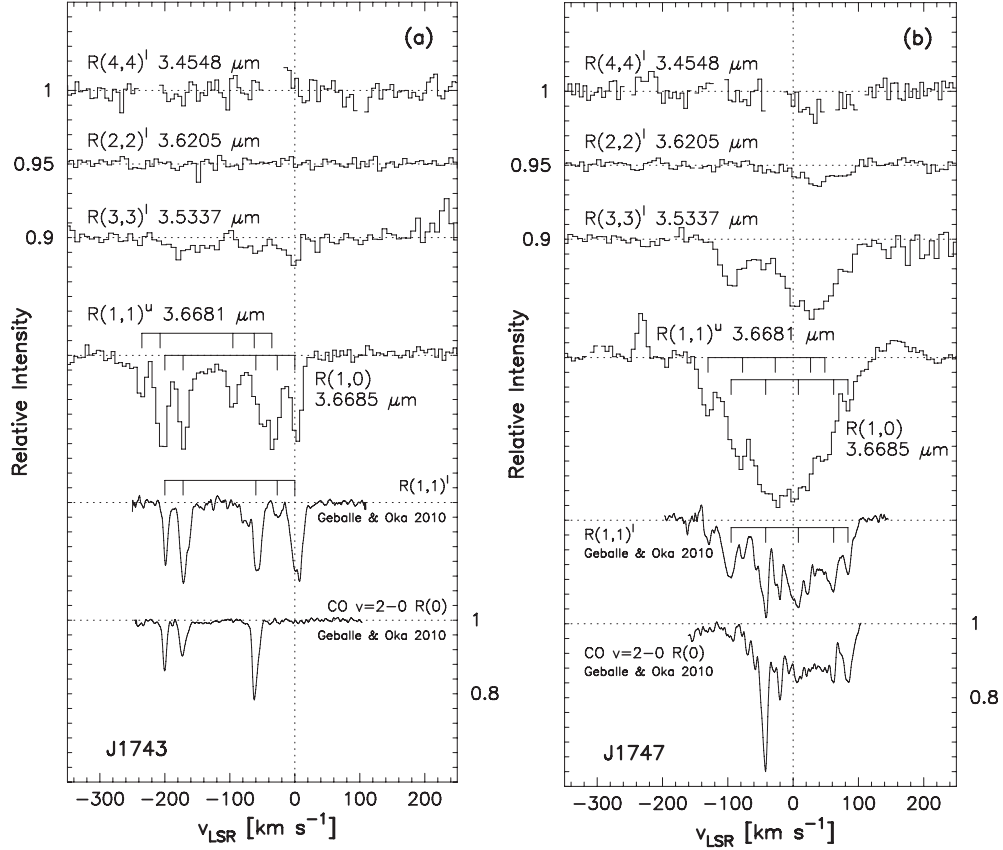


Fig. 1. Left (a): the spectra of H_3^+ at $R(4,4)^l$, $R(2,2)^l$, $R(3,3)^l$, and $R(1,0)$ [overlapped with $R(1,1)^u$] in the line of sight to 2MASS J17432173–2951430. H_3^+ $R(1,1)^l$ and CO $R(0)$ lines are taken from Geballe and Oka (2010). Right (b): the same as at the left, but for 2MASS J17470898–2829561. The velocities marked by the five vertical lines are 0, -27 , -60 , -172 , and -200 km s^{-1} for J1743 and 84, 62, 8, -42 , and -95 km s^{-1} for J1747.

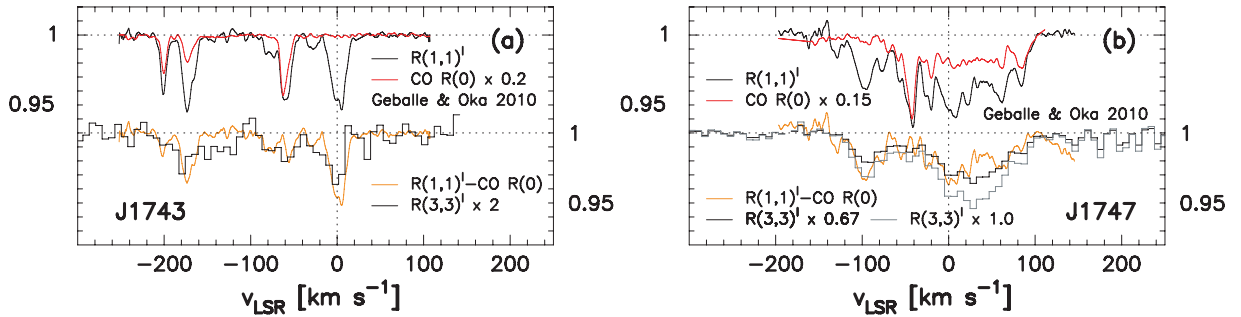


Fig. 2. Left (a): $R(1,1)^l$ and CO $R(0)$ spectra of 2MASS J17432173–2951430 taken from Geballe and Oka (2010). CO $R(0)$ is scaled by a factor of 0.2 so that the sharp absorption lines at -60 km s^{-1} are almost the same in depth. The difference of the two spectra is shown in orange (or thin line) in the lower trace to compare it with the $R(3,3)^l$ spectrum obtained in this study. The $R(3,3)^l$ spectrum is scaled by 2 to match the differential spectrum of $R(1,1)^l$ and CO $R(0)$. Right (b): the same as at the left, but for 2MASS J17470898–2829561. CO $R(0)$ is scaled by 0.15 so that the absorption line at -42 km s^{-1} has roughly the same depth as $R(1,1)^l$. The differential spectrum of $R(1,1)^l$ and CO $R(0)$ is compared in the lower trace. $R(3,3)^l$ and the differential spectrum at > -60 km s^{-1} after scaling by 0.67 (black trace) match well, while the scaling factor is close to unity at < -60 km s^{-1} (gray trace).

-172 km s^{-1} . The two cloud components with the high negative velocities of -200 km s^{-1} and -172 km s^{-1} are due to local dense clouds in Sgr E, as previously observed by Liszt (1992).

The spectra of J1747 follow the same pattern. In the upper traces of figure 2b, we show the H_3^+ $R(1,1)^l$ and CO $2-0$ $R(1)$ lines in J1747 (Geballe & Oka 2010), after rescaling the CO line by a factor of 0.15, so that the common absorption

components at -42 km s^{-1} , which probably arise in dense cloud material in the foreground 3 kpc spiral arm, have the same depth. The absorption by CO $v = 2-0$ at negative velocities is cut off at -60 km s^{-1} , unlike the absorption by H_3^+ $R(1,1)^l$, which extends to -150 km s^{-1} . The absorptions by H_3^+ $R(1,1)^l$ and CO have similar extents at positive velocities, but that of H_3^+ is much stronger than CO $v = 2-0$ after

Table 2. Column densities of H_3^+ toward 2MASS J1747 and 2MASS J1743.

	Δv^* [km s $^{-1}$]	$N(1,1)$ [10^{14}cm^{-2}]	$N(3,3)$ [10^{14}cm^{-2}]	$N(2,2)^\S$ [10^{14}cm^{-2}]	$N(4,4)^\S$ [10^{14}cm^{-2}]	$n(3,3)/n(1,1)$	$n(3,3)/n(2,2)$	$n(\text{H}_2)$ [cm^{-3}]	$T(\text{H}_2)$ [K]
2MASS J17470898–2829561	–150, –60 † –60, +100 ‡	6.0 ± 0.7 16.4 ± 1.2	4.3 ± 1.3 18.2 ± 2.2	< 0.8 5.8 ± 1.5	< 1.8 < 3.3	0.7 ± 0.2 1.1 ± 0.2	> 5.4 3.1 ± 0.9	< 50 $100\text{--}150$	$200\text{--}350$ $300\text{--}400$
2MASS J17432173–2951430	–220, +20	12.8 ± 1.9	5.7 ± 2.2	< 2.1	< 5.0	0.45 ± 0.2	> 2.9	< 50	$150\text{--}250$

* The interval that the column densities are calculated.

† The CMZ component.

‡ Sgr B component.

§ The upper limits are for 1σ .

scaling. Again the $R(3,3)^l$ profile reproduces the extra absorption of $R(1,1)^l$ well, with two broad absorption components, from -120 to -60 km s $^{-1}$ and from -60 to 100 km s $^{-1}$. The rule that CO and H_3^+ $R(3,3)^l$ separately trace dense and diffuse gas in a line of sight, respectively, while $R(1,1)^l$ traces both of them (Oka et al. 2005), thus also applies to J1743 and J1747. This consistency lends support to the idea that the warm and diffuse clouds found on sightlines within 30 pc of the Galactic nucleus are present ~ 100 pc apart from it.

A closer examination of the J1747 data reveals that the scaling factor of $R(3,3)^l$ at < -60 km s $^{-1}$ needed to match $R(1,1)^l$ is slightly different from that at > -60 km s $^{-1}$. The $R(1,1)^l - \text{CO } R(0)$ difference spectrum matches the $R(3,3)^l$ at > -60 km s $^{-1}$ when scaling $R(3,3)^l$ by 0.67 (black trace in figure 2b), while the scaling factor at < -60 km s $^{-1}$ is close to unity (gray trace). This is most simply interpreted as being a temperature effect. The > -60 km s $^{-1}$ absorption probably localizes on the Sgr B star-forming region (Geballe & Oka 2010), as is seen in the broad and strong absorption of CO $v = 2-0$. We infer that the absorbing gas in Sgr B is warmer, and thus produces a higher $n(3,3)/n(1,1)$ ratio. The < -60 km s $^{-1}$ absorption probably arises in the somewhat cooler diffuse clouds elsewhere in the CMZ.

The equivalent widths of the absorption lines in the warm and diffuse gas were converted to the column densities in the $v = 0$ (1, 1), (2, 2), and (3, 3) levels in the same manner as Geballe et al. (1999) and Goto et al. (2002). The squares of the transition dipole moments used for $R(1,1)^l$, $R(2,2)^l$, $R(3,3)^l$, and $R(4,4)^l$, which are 0.0141, 0.0177, 0.0191, and 0.0198 D 2 , respectively, are based on the Einstein A coefficients given in Neale, Miller, and Tennyson (1996). The densities and the temperatures of the absorbing clouds were determined from the relative populations of H_3^+ in $(J, K) = (1, 1)$, (2, 2), and (3, 3), by using the steady state model of Oka and Epp (2004). The detection of the $R(2,2)^l$ line toward J1747, only the second detection of this line, allows the density in this sightline to be determined, rather than an upper limit. The results are given in table 2. Figure 3 shows the temperature distribution in the CMZ as a function of the distance from the Galactic nucleus. The cloud temperatures observed so far in the CMZ are in the 100–400 K range. There is some possibility that the temperatures are lower in the line of sight to J1743 than elsewhere.

4. Discussion

The region containing warm and diffuse gas is now 7 times more extensive in Galactic longitude than originally found by

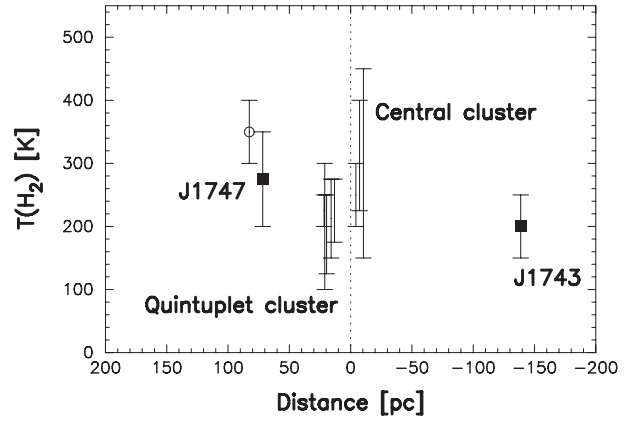


Fig. 3. Temperature distribution in the CMZ as a function of the distance from the Galactic nucleus. The distance to the Galactic center is assumed to be 7.6 kpc. The data for the Central cluster and the Quintuplet cluster are taken from Goto et al. (2008). The filled squares are of the present study. The open circle is for the positive velocity component in 2MASS J17470898–2829561, which is likely locally associated with the Sgr B star-forming region.

Goto et al. (2008). This environment is exclusive to the CMZ of the Galactic center, as $R(3,3)^l$ has not been detected in the clouds in the Galactic disk. How far beyond a radius of 100 pc the outer boundary of the cloud is yet to be determined. Although the observations reported in this paper are only toward two stars, one 130 pc West and the other 80 pc East, additional observations toward several other stars between them (T. Oka et al. in preparation) yield comparable column densities of H_3^+ in warm- and low-density clouds, further suggesting that this environment exists throughout the CMZ with a large volume filling factor.

The recent detections of strong far-infrared absorption by H_2O^+ toward Sgr B2 (Schilke et al. 2010) using the HIFI instrument on the Herschel Space Observatory have given independent evidence for the existence of a large amount of diffuse gas in the CMZ. Because H_2O^+ is produced from OH^+ through the hydrogen-abstraction reaction $\text{OH}^+ + \text{H}_2 \rightarrow \text{H}_2\text{O}^+ + \text{H}$, and OH^+ is produced either from O^+ by the hydrogen-abstraction reaction $\text{O}^+ + \text{H}_2 \rightarrow \text{OH}^+ + \text{H}$, or from O by the proton-hop reaction $\text{O} + \text{H}_3^+ \rightarrow \text{OH}^+ + \text{H}_2$, H_2O^+ is closely related chemically to H_3^+ . H_2O^+ is rapidly destroyed by H_2 through the hydrogen-abstraction reaction $\text{H}_2\text{O}^+ + \text{H}_2 \rightarrow \text{H}_3\text{O}^+ + \text{H}$, so it cannot be abundant in dense clouds. Gerin et al. (2010) and Neufeld et al. (2010), who observed

strong absorption by both OH^+ and H_2O^+ toward W 31 C and W 49 N, respectively, have concluded from chemical analysis that these molecular ions are found in diffuse gas with a very low fraction of molecular hydrogen, $f(\text{H}_2)$. Unlike H_3^+ , they cannot be used to determine temperatures directly because, due to their large dipole moments, only the lowest levels are populated. The “spin” temperature determined from the observed ortho to para ratio of H_2O^+ is not straightforward to interpret in terms of a kinetic temperature. Gerin et al. (2010) estimate to be $T \sim 100$ K.

In addition to the chemical connection between H_2O^+ and H_3^+ , there is some direct observational evidence that the two species are colocated. The velocity profiles of ortho- and para- H_2O^+ reported by Schilke et al. (2010) (see their figures 1 and 2) are remarkably similar to the H_3^+ velocity profile toward J1747 of Geballe and Oka (2010) reproduced in figures 1 and 2 of this paper. Not only do both range from ~ -120 km s^{-1} to ~ 90 km s^{-1} , but also the velocities of individual peaks approximately match. The identical peaks at -48 km s^{-1} , -26 km s^{-1} , and 4 km s^{-1} , which are due to the three foreground spiral arms, are not surprising. However, the absorption peaks near -100 km s^{-1} and 60 km s^{-1} , which are due to gas within the GC, also match (Oka 2010). Similar agreement is observed between the velocity profiles of $^{13}\text{CH}^+$ (E. Falgarone, private

communication) and H_3^+ . We regard these as strong indications that H_2O^+ , CH^+ and H_3^+ are largely found together. This is somewhat surprising, since H_2O^+ and CH^+ require low $f(\text{H}_2)$, while H_3^+ favors high $f(\text{H}_2)$. The locations of Sgr B2 and J1747 are separated in the plane of the sky by 16 pc. The velocity correspondence may be due to the large extents of diffuse clouds within the Sgr B complex.

We thank the staff of the Subaru Telescope and National Astronomical Observatory of Japan for invaluable assistance in obtaining these data. This research made use of the SIMBAD database, operated at CDS, Strasbourg, France. We also thank the referee, J. H. Black, for suggesting that we discuss relevant results from the Herschel Observation. T. R. G.’s research is supported by the Gemini Observatory, which is operated by the Association of Universities for Research in Astronomy, Inc., on behalf of the international Gemini partnership of Argentina, Australia, Brazil, Canada, Chile, the United Kingdom, and the United States of America. B. J. M. and N. I. have been supported by NSF Grant PHY 08-55633. T. O. acknowledges NSF Grant AST 08-49577. We appreciate the hospitality of the local Hawaiian community that made possible the research presented here.

References

- Eisenhauer, F., et al. 2005, *ApJ*, 628, 246
 Geballe, T. R., McCall, B. J., Hinkle, K. H., & Oka, T. 1999, *ApJ*, 510, 251
 Geballe, T. R., & Oka, T. 2010, *ApJ*, 709, L70
 Gerin, M., et al. 2010, *A&A*, 518, L110
 Goto, M., et al. 2008, *ApJ*, 688, 306
 Goto, M., McCall, B. J., Geballe, T. R., Usuda, T., Kobayashi, N., Terada, H., & Oka, T. 2002, *PASJ*, 54, 951
 Indriolo, N., Geballe, T. R., Oka, T., & McCall, B. J. 2007, *ApJ*, 671, 1736
 Kobayashi, N., et al. 2000, *Proc. SPIE*, 4008, 1056
 Liszt, H. S. 1992, *ApJS*, 82, 495
 Lord, S. D. 1992, A New Software Tool for Computing Earth’s Atmosphere Transmissions of Near- and Far-Infrared Radiation, NASA Technical Memoir 103957 (Moffett Field, CA: NASA Ames Research Center)
 McCall, B. J., et al. 2002, *ApJ*, 567, 391
 McCall, B. J., Geballe, T. R., Hinkle, K. H., & Oka, T. 1999, *ApJ*, 522, 338
 Morris, M., & Serabyn, E. 1996, *ARA&A*, 34, 645
 Neale, L., Miller, S., & Tennyson, J. 1996, *ApJ*, 464, 516
 Neufeld, D. A., et al. 2010, *A&A*, 521, L10
 Nishiyama, S., et al. 2006, *ApJ*, 647, 1093
 Oka, T. 2010, in *AIP Conf. Proc.*, Spectroscopy of Molecular Ions in the Laboratory and in Space (New York: AIP) in press
 Oka, T., & Epp, E. 2004, *ApJ*, 613, 349
 Oka, T., Geballe, T. R., Goto, M., Usuda, T., & McCall, B. J. 2005, *ApJ*, 632, 882
 Pan, F.-S., & Oka, T. 1986, *ApJ*, 305, 518
 Ramírez, S. V., Arendt, R. G., Sellgren, K., Stolovy, S. R., Cotera, A., Smith, H. A., & Yusef-Zadeh, F. 2008, *ApJS*, 175, 147
 Schilke, P., et al. 2010, *A&A*, 521, L11